

IMPEDANCE MINIMIZATION BY NONLINEAR TAPERING

Boris Podobedov[#], BNL/NSLS, Upton, New York, USA

Igor Zagorodnov[&], DESY, Hamburg, Germany

Abstract

There exist analytical approximations that express the transverse geometric impedance of tapered transitions in the inductive regime as a functional of the transition boundary and its derivatives. Assuming the initial and final cross-sections and the transition length are fixed, one can minimize these functionals by appropriate choice of the boundary variation with the longitudinal coordinate. In this paper we numerically investigate how well this works for the cases of optimized tapered transitions in circular, elliptical and rectangular geometry by running ABCI, ECHO, and GdfidL EM field solvers. We show that a substantial reduction of impedance for optimized boundary compared to that of a linear taper is indeed possible in some cases, and then we compare this reduction to analytical predictions.

INTRODUCTION

Yokoya has derived the low frequency transverse impedance of an axially symmetric tapered transition [1],

$$Z_{\perp}(k) \cong -\frac{iZ_0}{2\pi} \int_{-\infty}^{\infty} dz \frac{r'(z)^2}{r(z)^2}, \quad (1)$$

where k is the wavenumber of the perturbing field, Z_0 the free space impedance, $r(z)$ the radius of the tapered circular chamber, and prime denotes derivative with respect to z . He has also pointed out that when a transition between the minimum and the maximum radii (r_{\min} and r_{\max}) occurs over a length L , the exponential boundary

$$r_{\exp}(z) = r_{\min} \times \alpha^{z/L}, \quad \alpha \equiv r_{\max} / r_{\min} \quad (2)$$

minimizes the resulting impedance ($Z_{\perp_{\exp}}$) such that

$$Z_{\perp_{\exp}} / Z_{\perp_{lin}} = \text{Log}^2(\alpha) [\alpha + \alpha^{-1} - 2]^{-1}, \quad (3)$$

$$\text{where } Z_{\perp_{lin}} = -iZ_0 [2\pi L]^{-1} (\alpha + \alpha^{-1} - 2) \quad (4)$$

is the impedance due to a linearly tapered boundary

$$r_{lin}(z) = r_{\min} (1 + (\alpha - 1) \times z / L). \quad (5)$$

As per Eq. (3) a large reduction in impedance by going from linear to exponential taper occurs only in cases of very large radial variations (e.g. a factor of 2 impedance reduction for $\alpha=20$).

Stupakov [2] re-derived Eq. (1) by a different technique and proved that it is valid all the way down to $k=0$. Using this technique, Stupakov [3] also determined the vertical

[#]Work supported by DOE contract number DE-AC02-98CH10886.

[&]Work supported by EU contract 011935 EUROFEL

(dipolar) impedance of a flat rectangular chamber of constant half-width w and varying half-height $h(z) \ll w$,

$$Z_y^{rect}(0) = -\frac{iZ_0 w}{4} \int_{-\infty}^{\infty} dz \frac{h'(z)^2}{h(z)^3}, \quad (6)$$

which amounts to a much larger impedance than Z_{\perp} for a round chamber of the same vertical profile, $r(z)=h(z)$.

Recently, Podobedov and Krinsky calculated low frequency transverse impedances for a gradual taper with elliptical cross-section [4-5]. In the inductive regime and large horizontal-to-vertical aspect ratio, $w/h \gg 1$ these (dipolar) impedances could be expressed as

$$Z_x^{ell}(k) \cong -\frac{iZ_0}{4\pi} \int_{-\infty}^{\infty} dz \frac{h'(z)^2}{h(z)^2}, \quad k \leq 1/h_{\min}, \quad (7)$$

$$Z_y^{ell}(k) = -\frac{iZ_0 \pi w}{16} \int_{-\infty}^{\infty} dz \frac{h'(z)^2}{h(z)^3}, \quad k \leq 1/w, \quad (8)$$

where $h \ll L$ in Eq.(7), and $w \ll L$ in Eq. (8). While these expressions were derived for confocal elliptical boundary, they are expected to approximately hold in general, if the above assumptions are held. Since the functional Eq. (7) is of the same form as Eq. (1) the optimizing boundary given by Eq. (2) (with r replaced by h) applies directly to the horizontal impedance. By analogy with Eq. (3) we expect large horizontal impedance reduction only in cases of very large height variation $h_{\max}/h_{\min} \gg 1$.

On the other hand, for the vertical impedance minimizing the functional Eq. (8) (or Eq. (6)) we obtain the boundary

$$h_{optZy}(z) = \frac{h_{\min}}{(1 + (\beta^{-1/2} - 1)z/L)^2}, \quad \beta \equiv h_{\max} / h_{\min}, \quad (9)$$

with the corresponding impedance, $Z_{y_{opt}}$,

$$Z_{y_{opt}} / Z_{y_{lin}} = 8 \beta (1 + \beta^{1/2})^{-2} (1 + \beta)^{-1}, \quad (10)$$

reduced more effectively than in the horizontal case, e.g. Eq. (10) gives a factor of 2 reduction in Z_y for $\beta=7.6$.

The optimizing boundaries given by Eq. (2) and Eq (9) are qualitatively similar. Compared to the linear case both have reduced slope when $h(z)$ is small and vice-versa. Therefore, using optimal tapering Eq. (9) to minimize Z_y should lower Z_x as well; similarly Eq. (2) boundary not only minimizes Z_x but results in lower Z_y as well.

Eq. (1) and Eqs. (6-8) have been derived under several restrictive conditions. Impedance reduction, Eq. (3) and Eq. (10), should therefore be regarded as approximate. To

independently probe their accuracy we have performed numerical calculations using ABCI [6], ECHO [7], and GDFIDL[8] EM field solvers for tapered structures with round, elliptical and rectangular cross-sections.

We consider gradual tapers, $(h_{max}-h_{min})/L \ll 1$. For elliptical and rectangular structures we take the aspect ratio at the minimum cross-section of $w_{min}/h_{min} = 3$ or larger. Nonlinear boundary is approximated by a piecewise linear boundary. Bunch length is chosen to be mainly in the inductive impedance regime. The minimum radius r_{min} (or half-height h_{min} for 3D structures) is taken to be 1 cm for all calculations presented in this paper. Dual tapered structures of both convex (cavity-like) and concave (collimator-like) geometry have been used.

AXIALLY SYMMETRIC TAPERS

ECHO simulations were done for concave structures with $r_{max}=2, 6, 10, 14$ and 18 cm and $L=(r_{max}-r_{min}) \times 80/17$. ECHO results ($-\text{Im}[Z_{\perp}(0)]$), with estimated accuracy of $<1\%$, for linear taper are $1.12, 2.00, 2.20, 2.27$ and 2.31 $\text{k}\Omega/\text{m}$; exponential tapering values are $1.08, 1.58, 1.43, 1.31,$ and 1.20 $\text{k}\Omega/\text{m}$. These agree to $<12\%$ with Eq. (1) and are in perfect agreement with more precise analytical results of [9]. Impedance reduction ratio, plotted in Fig. 1, is in very good agreement with Eq. (3).

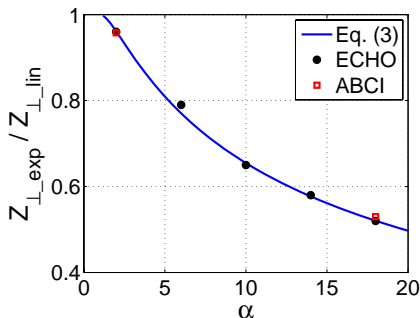


Figure 1: Z_{\perp} reduction due to Eq. (2) tapering.

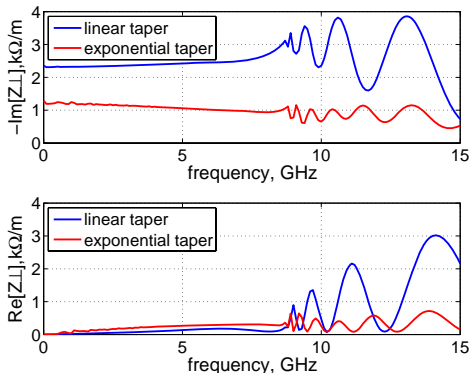


Figure 2: Z_{\perp} for Eq. (5) and Eq. (2) tapering, $\alpha=18$.

A separate set of calculations was done with ABCI for convex geometry, $\alpha=2$ ($L=5$ cm) and $\alpha=18$ ($L=80$ cm). Each geometry was calculated at several mesh sizes and results were extrapolated to zero mesh size to improve the accuracy (see Appendix of [9]). Impedance values agree well with ECHO; the ratio is shown in Fig. 1.

Finally, Fig. 2 shows impedances found by ECHO as a function of frequency for the case $\alpha=18$. Clearly, the reduction predicted by Eq. (3) for $\text{Im}[Z_{\perp}]$ holds in the inductive regime range, $k \ll 1/r_{min}$. $\text{Re}[Z_{\perp}]$ remains small for both linear and exponential tapers.

ELLIPTICAL TAPERS

GDFIDL was used to calculate impedances of convex structures with confocal (i.e. $w(z)^2-h(z)^2 = \text{const.}$) elliptical cross-section. Each taper was evenly sub-divided into 4 linearly tapered pieces. Three cases of $\beta=4.5, 9,$ and 18 (with $L=20, 46,$ and 96 cm) were calculated, with the smallest mesh size of $0.25, 0.25$ and 0.4 mm. As with ABCI we extrapolated impedance to zero mesh size. Results for $w_{min}/h_{min}=4$, given as $Z_x[\text{k}\Omega/\text{m}]/Z_y[\text{k}\Omega/\text{m}]$ are a) linear tapering: $0.626/3.03, 0.761/3.64, 0.895/3.88$; b) Eq. (2) tapering: $0.518/2.62, 0.548/2.28, 0.550/1.78$; c) Eq. (9) tapering: $0.528/2.54, 0.583/2.16, 0.641/1.65$.

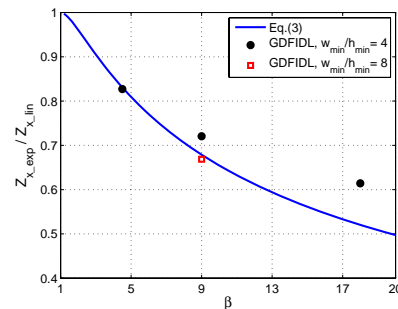


Figure 3: Z_x reduction due to Eq. (2) tapering.

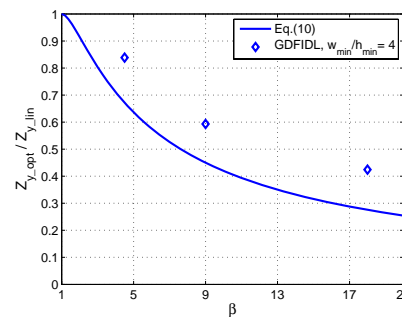


Figure 4: Z_y reduction due to Eq. (9) tapering.

Horizontal impedance is 10-20% lower than Eq. (7), it agrees better with more precise formulas of [4-5], that do not require $w/h \gg 1$. Disagreement for the vertical impedance and Eq. (8) is larger, especially at large β , possibly due to tapers not being sufficiently long and/or flat. The cause is currently under investigation.

Impedance reduction ratio is shown in Figs. 4-5. Substantial reduction is achieved for large β ; also we confirmed that both Z_x and Z_y reduce for either Eq. (9) or Eq. (2) tapering. As expected there is some disagreement with the theory, however for the horizontal it seems to disappear if we go to flatter tapers (see $w_{min}/h_{min} = 8$ point in Fig. 3). For the vertical the disagreement is more profound. Reduction factors due to exponential, Eq. (2),

and optimal vertical, Eq. (9), tapers are closer to each other than the theoretical predictions Eqs. (3) and (10).

Finally, Fig. 6 shows that Z_y reduction holds up to rather high frequencies $k \sim 1/w_{\min}$. We also confirmed that for Z_x it extends up to $k \sim 1/h_{\min}$.

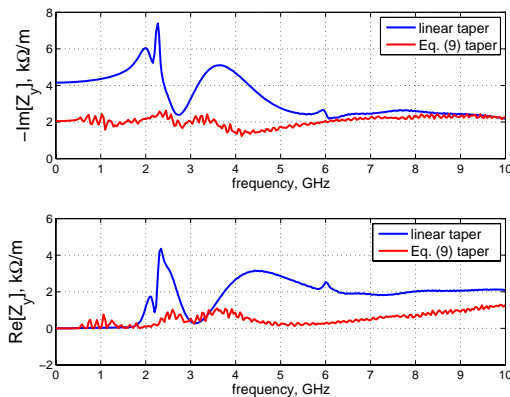


Figure 5: Z_y for Eq. (5) and Eq. (9) tapering, $\beta=18$.

RECTANGULAR TAPERS

Rectangular tapers of constant width were calculated in concave geometry. Maximum height was adjusted as shown in Table 1, maximum cross-section had a square shape, $w=h_{\max}$; additionally $w/h_{\max}=2$ case was calculated at $\beta=5$. Taper length was taken from $L=(h_{\max}-h_{\min}) \times 80/17$. Calculations were done with 1 mm mesh size. To check the accuracy we repeated the ECHO run for $\beta=5$, Eq. (9) taper, with 0.5 mm mesh, and the wake-potentials came out virtually the same. Similar to the elliptical case we obtain Z_y much smaller than analytic predictions (see Table 1). Z_y reduction ratios shown in Fig. 6 are higher than Eq. (10). Flattening the structure (L fixed) makes the vertical reduction ratio disagree even more. On the contrary, for the horizontal impedance we observe better agreement with Eq. (3). It improves even further for flatter tapers.

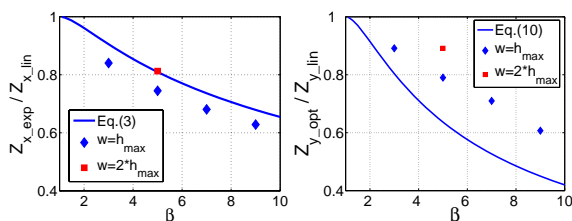


Figure 6: Z_x reduction due to Eq. (2) tapering (left) and Z_y reduction due to Eq. (9) tapering.

Table 1. Z_y values from ECHO and (parenthesis) Eq. (6).

h_{\max} , cm	$Z_{y, \text{lin}}$, k Ω /m	$Z_{y, \text{opt}}$, k Ω /m	$Z_{y, \text{opt}}/Z_{y, \text{lin}}$
3	3.25 (5.3)	2.90 (4.3)	0.89
5	5.62 (9.6)	4.44 (6.1)	0.79
7	7.70 (13.7)	5.50 (7.2)	0.70
9	10.1 (17.8)	6.1 (8.0)	0.60

CONCLUSION

By running extensive simulations with EM field solvers ABCI, ECHO, and GDFIDL we have investigated the effectiveness of non-linear tapering to further reduce low frequency broadband transverse geometric impedance of gradual tapers as compared to a linear tapering. For transitions with large cross-sectional changes optimal nonlinear tapering does provide large reduction in transverse impedance. Exponential tapering of the radial boundary, Eq. (2), reduces Z_{\perp} for axially symmetric case; the same tapering in the vertical profile reduces Z_x (for 3D flat tapers). For a factor of 20 change in r (or h for 3D) a factor of two impedance reduction is possible. For these two cases theoretical predictions for impedance reduction as well as the absolute values of the impedance, agree well with simulations. On the other hand, the vertical impedance simulations indicate that while the boundary given by Eq. (8) reduces Z_y by a slightly larger factor than what Eq. (2) achieves for Z_x , the reduction falls short of theoretical predictions. We note that for the geometries we considered, the values of Z_y for a linear taper were lower than what is given by Eq. (6) and Eq. (8) due to tapers not being sufficiently long and/or flat, or possibly due to other factors. Simulations for longer and flatter tapers are now in progress.

We found that for flat 3D case optimal tapering for one plane reduces the impedance in the other plane. Additionally, we established that impedance reductions, predicted from zero-frequency considerations, hold well up to frequencies $k \sim 1/w_{\min}$ (Z_y), $k \sim 1/h_{\min}$ (Z_x), and $k \sim 1/r_{\min}$ (Z_{\perp}). Also, we observed very similar impedance behaviour for rectangular and elliptical structures, as well as established that piece-wise linear tapering with only a few linear segments (which would be easier to manufacture) works almost as effectively as a full non-linear tapering. Finally, we note that in the common practical case when the end cross-sections and transition lengths are fixed, and the small cross-section is relatively flat, the vertical profile tapering considered in this paper is the only way to reduce the low frequency broad-band geometric impedance.

We acknowledge insightful discussions with S. Krinsky and G.V. Stupakov. We thank W. Bruns, A. Blednykh, and P.J. Chou for help with GDFIDL. We also thank CST GmbH for letting us use CST Microwave Studio for mesh generation for ECHO simulations.

REFERENCES

- [1] K. Yokoya, CERN SL/90-88 (AP), 1990
- [2] G.V. Stupakov, PAC-2001, p.1859
- [3] G.V. Stupakov, SLAC-PUB-7167, 1996
- [4] B. Podobedov, S. Krinsky, EPAC-2006, p. 2973
- [5] B. Podobedov, S. Krinsky, accepted PRST-AB, 2007
- [6] Y.-H. Chin, CERN SL/94-02 (AP), 1994
- [7] I.Zagorodnov, T. Weiland, PRST-AB **8**, 042001, 2005
- [8] W. Bruns, <http://www.GdfidL.de>
- [9] B. Podobedov, S. Krinsky, PRST-AB **9**, 054401, 2006